



Lawrence Berkeley Laboratory

UNIVERSITY OF CALIFORNIA

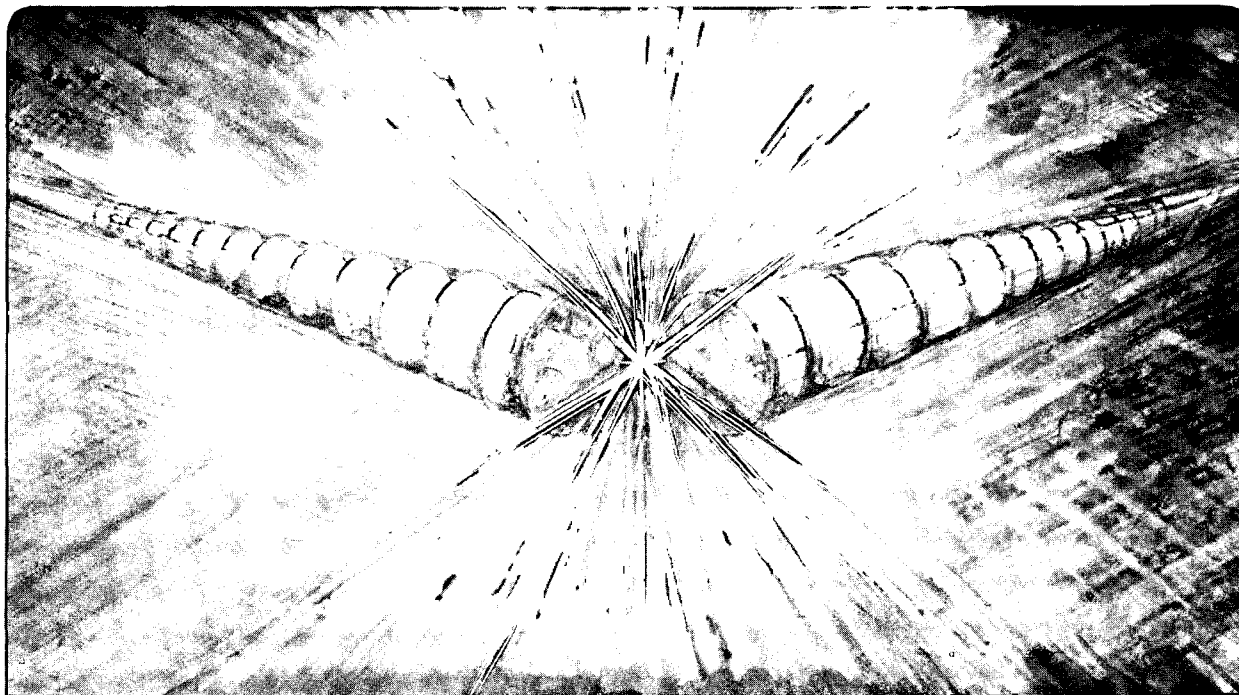
Accelerator & Fusion Research Division

Presented at the IIT/94 Conference, Catania, Italy, June 13-17, 1994,
and to be published in the Proceedings

Surface Charge Control During High-Current Ion Implantation: Characterization with CHARM-2 Sensors

M.I. Current, W. Lukaszek, M.C. Vella, and N.H. Tripsas

June 1994



REFERENCE COPY	_____
Does Not Circulate	_____
Copy 1	_____
Bldg. 50 Library.	

LBL-35963

DISCLAIMER

This document was prepared as an account of work sponsored by the United States Government. While this document is believed to contain correct information, neither the United States Government nor any agency thereof, nor the Regents of the University of California, nor any of their employees, makes any warranty, express or implied, or assumes any legal responsibility for the accuracy, completeness, or usefulness of any information, apparatus, product, or process disclosed, or represents that its use would not infringe privately owned rights. Reference herein to any specific commercial product, process, or service by its trade name, trademark, manufacturer, or otherwise, does not necessarily constitute or imply its endorsement, recommendation, or favoring by the United States Government or any agency thereof, or the Regents of the University of California. The views and opinions of authors expressed herein do not necessarily state or reflect those of the United States Government or any agency thereof or the Regents of the University of California.

IIT/94, Catania, Italy, June 13-17

Rev 4.0 Thu., Aug. 18, 1994

Surface Charge Control During High-Current Ion Implantation: Characterization with CHARM-2 Sensors

Michael I. Current,^a Wes Lukaszek,^b Michael C. Vella,^{c,*} Nicholas H. Tripsas^d

^aApplied Materials, Implant Division, Santa Clara, CA 95054 USA

^bWafer Charging Monitors, Woodside, CA 94062 USA

^cLawrence Berkeley Laboratory, Berkeley, CA 94720 USA

^dAdvanced Micro Devices, Sunnyvale, CA 94088 USA

Abstract

Studies of the charging effects during implantation with 9200 and 9500 tools using EEPROM-based sensors, CHARM-2, are reported for 60keV As beams.

1. Introduction

The thinning of gate oxides for advanced MOS devices has increased the sensitivity of these oxides to excessive charge flows and potentials during exposure to ion beam processing. Tracking the intrinsic breakdown voltage of SiO₂ as $\approx 10\text{MV/cm}$, this corresponds to a $\pm 10\text{V}$ limit for gate-to-substrate potentials for 100Å oxides (Fig.1). This sensitivity is further tightened by concern for pre-breakdown damage (generated by current flows at potentials greater than $\approx 50\%$ of breakdown conditions) as well as charge sharing and current funneling effects of long-line gate-interconnect structures [1,2]. The reduction of intrinsic breakdown voltage has driven the development of supplemental electron sources with ever-decreasing electron energies and increased coupling to the ion beam plasma (Fig.1).

Additional progress towards charge control has been limited by the lack of detailed understanding of the interaction of the ion beam plasma with device structures on the wafer surface [3,4]. If the ion beam is interpreted as a plasma of some complexity [5], a variety of charged species must be considered (Fig. 2). In addition to the energetic dopant ions, the ion beam plasma contains a significant number of "slow ions", created by collisions between the energetic dopant ions and

*On leave from the Lawrence Berkeley Laboratory, MS 47-112, Berkeley, California 94720, USA. This work partially supported by the Director, Office of Energy Research, Office of Fusion Energy, Development and Technology Division, of the U.S. Department of Energy under Contract No. DE-AC03-76SF00098.

background gas atoms in the beam path [6]. Other ionized species include ions from wafer charge control systems, such as "plasma bridge" devices [7], sputtered ions from bombarded surfaces in the implanter and charged species generated by the decomposition of photoresist during the early stages of the implant cycle.

The electron population is essentially equal to the density of the total ion species in the regions of the beamline where the absence of acceleration fields allow for quasi-neutrality of the beam plasma. The electron energy spectra is however quite complex. Those electrons which are trapped in the ion beam column have energies of the order of the beam potential while the energies of electrons which enter the ion beam plasma from a wafer charge control system are determined by the local potentials in the charge control device [3].

2. Test Structures for Surface Potential and Charge Flows: CHARM-2

Device-scale sensors using EEPROM-based structures (Fig. 3) for measurement of surface potentials and net charge flows provide a new and detailed view of plasma conditions on the wafer surface during implantation. CHARM-2 (CHARGE Monitor) devices [8-11] use large-area Al electrodes tied to the control gate of an EEPROM transistor to sense the local surface potential. Electrodes which are tied to the Si substrate through poly-Si resistors measure the net charge flux on the electrode. Voltages and currents on the wafer surface are inferred from shifts in the transistor threshold voltage after exposure to an ion beam process environment.

Many of the charge collection electrodes are connected to the Si wafer substrate through poly resistors. Low-resistance shunts are used for structures which monitor the effects of uv-light from the ion beam plasma on uv-assisted charge transport in oxides. High-resistance electrode-to-substrate connections are used to monitor charge flux through the effect on the EEPROM of the voltage drop across the resistor. The range of charge flux that can be sensed by the CHARM-2 devices span from $0.1\text{A}/\text{cm}^2$ (using the full dynamic range of the threshold voltage swing (24V) and a $10^5 \Omega$ load resistor) to $\approx 8\mu\text{A}/\text{cm}^2$ (assuming a measurement resolution on the threshold voltage of $\leq 2\text{V}$)(Fig. 4).

The CHARM-2 device array includes a variety of structures designed to differentiate between a number of competing paths for charge flows in the device wafer. For example, lateral current paths along the wafer surface are monitored with antenna structures which are surrounded by guard-rings which are tied to the Si substrate and separated from the antenna edge by gaps ranging from 3 to 30 μ m. Antenna structures which are tied to the Si substrate through p⁺ or n⁺ diodes record the largest signals, of positive or negative polarity, encountered during the ion beam exposure. This memory capability is particularly important in processes where transients effects are significant; such as photoresist outgassing and carbonization during the early stages of high-dose implants.

3. Ion Implantation Studies

Using CHARM-2 monitors which were fabricated on 150mm wafers, the charging characteristics of 9200 and 9500 implanters were investigated under conditions typical of source/drain implantation. The wafers were electrically programmed and calibrated prior to implantation. The CHARM wafers were implanted with 16mA As beams at an energy of 60keV to a dose of 4.5x10¹⁵ As/cm². The As beam profiles were measured before implantation with a full width at half maximum of the beam current density of 68mm for both tools.

The Al charge collection electrodes and the top oxide surface were "dry", that is, free of any photoresist material. Earlier investigations with CHARM-2 devices on 100mm wafers [10] had shown that photoresist layers, particularly when placed over the charge collection electrodes, have a dramatic effect on the magnitude of positive charging signals. However, in the present study we wanted to investigate the use of CHARM as a monitor of tool performance for benchmarking and process control applications. For these applications, fast cycling of the CHARM monitors through the implantation tool and probe station is of prime importance, without the complications and delay of photoresist patterning and removal.

The charge control systems on the 9200 and 9500 were sampled for "typical" operating conditions. With the electron shower on the 9200, a dilute plasma is generated by electron collisions with Ar gas atoms that are flowing in the filament-grid electron source. The resulting plasma is loosely coupled to the ion beam plasma and low energy electrons are transported along the ion beam plasma to the wafer

surface. For these tests, electron shower was operated with an emission current of 200mA, filament bias voltage of 70V and an Ar gas flow of 1.42 sccm. With this Ar flow, the pressure in the wheel chamber was 1.7×10^{-5} torr.

The 9500 was fitted with a Plasma Flood Source [7] which consists of a sequestered arc chamber above the ion beam plasma and a guide tube box through which the ion beam passes just before arriving at the wafer surface. An Ar arc discharge is maintained in arc chamber by a 30V filament-to-arc chamber wall voltage. The arc discharge plasma flows out of the arc chamber through a circular opening and strongly couples to the ion beam plasma directly below it. The addition of the arc discharge plasma significantly increases the plasma density in the ion beam, which, among other effects, lowers the plasma potential of the beam [5,6,12].

The plasma flood source on the 9500 was tested in two operating modes; one where the filament was tied to the reference ground of guide tube wall ("accel/decel" mode) and one where the filament was floated above the local ground of the guide tube wall by the 30V arc discharge voltage ("bias" mode) [12]. In addition, the guide tube walls can be biased negative to the arc discharge plasma to increase the confinement of low energy electrons in the ion beam plasma. A guide tube bias of -10V was used in these tests.

4. Results from CHARM Sensor Measurements

After implantation, the threshold voltages of the CHARM EEPROM transistors were measured. By comparison to the gate voltage-threshold voltage calibration curves, the voltage on the charge collection electrodes were derived from the shifts in transistor threshold voltages.

Wafer maps of the positive charging current signal measured at 188 sites over the wafer (Fig. 5) show transient effects as the wafer passes into and out of the ion beam plasma for cases of the "raw" 16mA As beam (charge control system off). These "bow and stern" patterns were not reported in earlier studies [13,14] of charging effects in 9000 implanters using similar EEPROM-based sensor and mapping techniques. Although, significant wafer-edge transient effects have been reported for native (no electron shower) 30keV, 2mA As beams on a NV-80SD [18]. In previous studies with an NV-10 implanter [10], the spatial variation of the CHARM

sensor results resembled a “bull’s-eye” pattern. The spatial variation of the CHARM sensor readings are much more clearly resolved with the larger number of test sites and improved mapping techniques used in the present study.

The peak positive signals in the bow and stern regions are $\approx 5V$ higher than the overall wafer average of 11.8V. With the plasma flood system operated with a 6A arc discharge, the average surface charge is reduced to 6.74V and the peak positive charge is reduced to 10V. The bow and stern local transients were completely suppressed with the plasma flood source operated in the bias mode and with the 9200 electron flood shower.

The average positive potentials for these test conditions (Fig. 6) show the ability of the charge control systems on both 9200 and 9500 implanters to bring positive charging levels to $\leq +5V$ levels. The actual surface voltages may have been closer to zero than 5V, but this could not be resolved for the programming state values used in this study. The peak negative signal, measured on devices with floating charge collection electrodes, showed negative voltages ranging from -10 to -18V. The negative charge flux were at least an order of magnitude less than the positive currents (below the threshold for the CHARM current sensors). Earlier studies of charging effects in 9000 implanters with an EEPROM-based test device [13,14] linked strongly positive charging environments with increased oxide breakdown in test capacitors and showed only weak effects for negative charging conditions. These results are in good accord with this study.

5. Equivalent Circuit Models of Ion Beams, Electron Sources and Wafer Surfaces

The correlation of electrical data from EEPROM-like sensors with SPICE-based equivalent circuit models of plasma conditions has been successfully realized for several important plasma etching configurations[15]. The complications related to the strong transient effects involved with the scanning of the ion implantation beam over the wafer surface and the many charge exchange mechanisms between the wafer surface and beam plasma [3,4] have so far precluded modeling at a similar level of detail.

An approach [5] to modeling of the ion beam is to consider the charge flow onto the wafer surface to be a sum of current sources made up of the positive “fast” ion beam, j_{ib} , positive “slow” ions created by collisional ionization of background gases in the ion beam plasma, j_{ip} , and electrons coupled to the beam plasma, j_e (Fig. 7). The effect of the positive ion charging by the “fast” ion beam is enhanced by the ejection of secondary charges from the wafer surface so the net contribution is $j_{ib}(1 + \gamma_s)$, where γ_s is the secondary electron emission coefficient. The flow of plasma electrons to the wafer surface is $j_{ip} \exp[e(V_{device} - \phi_p)/kT_e]$, where V_{device} is the surface-to-substrate potential, ϕ_p is the plasma potential and T_e is the electron temperature. The voltage drop across an electrode-to-substrate resistor, R , is governed by the sum of the ion and electron contributions,

$$V_{device} = RA [j_{ip} \exp[e(V_{device} - \phi_p)/kT_e] + j_{ib}(1 + \gamma_s)] \quad (1)$$

where A is the area of the charge collection electrode.

The non-linear variation of the potential on charge collection electrodes with load resistance (Fig. 8) highlights the mixed behavior of the ion beam plasma as a current-voltage source. For low load impedance, the ion beam plasma acts as a current source following an Ohmic behavior with load impedance. At higher load impedances, the beam plasma clamps the surface potential at a value determined by the electron temperature. For the larger area electrodes, which collect more current, the saturation of the voltage source behavior occurs at lower load impedance. Effects of charge collection area have been reported for in-situ voltage sensors (with much large geometries) imbedded in wafer disks [16].

J-V characteristics

For the case of strong positive charging, a 16mA As beam with no electron shower, this plasma model [19] was fitted to the observed variation of the charge collection potential with load resistance. The circuit model values from a die showing strong positive signals (where the beam entered the wafer (Fig. 5a)) were $(j_{ib}/j_{ip}) = 11.8$, $T_e = 5.2\text{eV}$ and $j_{ib}(1 + \gamma_s) = 4.1 \text{ mA/cm}^2$. On a die near the center of the wafer, in the region where less positive charging was observed, (j_{ib}/j_{ip}) had decreased to 0.4. The equivalent load characteristics for these two cases (Fig. 9) show the shift in J-V characteristics with position on the CHARM wafer. Tunneling

current characteristic for 70 and 110Å oxides indicate that for these test conditions, no net current drive for tunneling-induced damage[17] for 110Å is present in the region where the transient effects are not important.

With the operation of the Plasma Flood System on the 9500 and the electron shower on the 9200, the maximum observed surface potentials were close enough to the $\pm 5V$ resolution limit set by the pre-programmed threshold voltages chosen for these tests that no significant positive current drives were observed. This implies that adequate charge control can be obtained with these systems for oxides at least as thin as 70Å.

6. Summary

CHARM-2 devices provide an direct view with unprecedented clarity of charge flux and potentials encountered by wafer surfaces exposed to ion beam processing environments. In these initial tests with 9200 and 9500 implanters, transient phenomena was observed near the wafer edges for 16mA As without use of charge control systems. These effects were analyzed in terms of the J-V characteristics of a the ion beam plasma. Further discussion of the plasma model is presented in Ref. 18. Follow-on work, utilizing EEPROM programing conditions which allow CHARM-2 devices to measure surface potentials closer to zero, is underway.

Acknowledgements:

We acknowledge the collaboration and support of Larry Larson at Sematech, Joe Reedholm at Reedholm Instruments, C. Messick, J. Shideler and S. Reno at National Semiconductor, H. Ito and J. England at Applied Materials.

Author notes:

* Partially supported by the Director, Office of Energy Research, Office of Fusion Energy, Development and Technology Division, of the U.S. Department of Energy under Contract No. DE-AC03-76SS00098.

References:

1. K.F. Schuegraf and C.-M. Hu, Proc. 1994 IEEE Inter. Reliability Physics Symp. (San Jose, CA, 1994)126-135.
2. W.M. Green and C.K. Lau, J. Electrochem. Soc.,**139** (1992) 2948-2952.

3. M.E. Mack, in **Handbook of Ion Implantation Technology**, ed. J.F. Ziegler, North-Holland, (1992) pp.599-646.
4. M.I. Current, A. Bhattacharyya and M. Khydr, *Nuc. Inst. Meth.* **B37/38** (1989) 555-558.
5. M. Vella, notes for UC Berkeley Extension Short Course on **Wafer Charging Effects in Ion Implantation Processing**, June 10-11, 1993, Dallas, TX. and LBL report LBL-34970 (1993).
6. J. England, N. Bryan, H. Ito, D. Armour, J. Van den Berg, I. Fotheringham and P. Kindersley, in **Ion Implantation Technology**, eds. D.F Downey, M. Farley, K.S. Jones and G. Ryding, Elsevier (1993) 613-616.
7. H. Ito, T. Kamata, J. England, I. Fotheringham, F. Plumb and M.I. Current, these proceedings.
8. W. Lukaszek, W. Dixon, E. Quek, W. Weisenberger and S. Ho, *Nuc. Inst. Meth.* **B74** (1993) 301-305.
9. W. Lukaszek and G. Angel, in **Ion Implantation Technology**, eds. D.F Downey, M. Farley, K.S. Jones and G. Ryding, Elsevier (1993) 645-650.
10. W. Lukaszek, W. Dixon, M.C. Vella, C. Messick, S. Reno and J. Schidler, *Proc. 1994 IEEE Inter. Reliability Physics Symp.* (San Jose, CA, 1994) 334-338.
11. M.I. Current, W. Lukaszek, W. Dixon, M.C. Vella, C. Messick, S. Reno, and J. Schidler, , in **Contamination Control and Defect Reduction in Semiconductor Manufacturing III**, *Electrochem. Soc. Proc.* 94-9 (1994) pp. 49-58.
12. J. England, C. Cook, D. Armour and M. Foad, these proceedings.
13. T. Namura, K. Ishikawa, N. Aoki, Y. Fukuzaki, Y. Todokoro and M. Inoue, *Japanese J. Appl. Phys.* **30** (1991) 3223-3227.
14. N. Aoki, K. Ishikawa, T. Namura, Y. Fukuzaki, G. Fuse, M. Yoshida and M. Inoue, *Nuc. Inst. Meth.* **B74** (1993) 306-310.
15. T. Namura, H. Uchida, H. Okada, A. Koshio, S. Nakagawa, Y. Todokoro and M. Inoue, in **Microelectronic Processing Integration '91**, SPIE (1991).
16. M.E. Mack, P. Barschall, P. Corey, S. Satoh and S. Walther, *Nuc. Inst. Meth.* **B74** (1993) 287-290.
17. P.P. Apte and K.C. Saraswat, *Proc. 1994 IEEE Inter. Reliability Physics Symp.* (IRPS), (San Jose, CA, 1994) 136-142.
18. Y. Sato, K. Anzai and F. Tadokoro, *IEEE Trans. on Semiconductor Manufacturing* **5**(4)(1992) 329-336 and **6**(3)(1993) 268-269.
19. M.C. Vella, W. Lukaszek, M.I. Current, N.H. Tripsas, these proceedings.

Figure Captions:

Fig. 1 Intrinsic breakdown voltage for gate oxide films and typical electron energy distributions for sequential generations of electron shower technologies.

Fig. 2 Charge exchange mechanisms on wafer surfaces and in ion beams.

Fig. 3. CHARM-2 EEPROM-based sensor device with resistor load for charge flux measurements.

Fig. 4 Charge flux density sensitivity ranges for CHARM-2 sensors for 2 and 24V voltage drops along poly-Si load resistors between charge collection electrodes and Si substrate (for 0.24mm^2 electrodes).

Fig. 5 Wafer maps of positive potential signal from CHARM-2 sensors for 16mA, 60keV As beams from a 9500 implanter. The surface potential for the "raw" As beam (no electron shower) (a) is $11.79\pm 2.74\text{V}$ and with the Plasma Flood Source (b) is 6.74 ± 0.636 . Note the transient effects that are resolved in these maps in the regions where the beam passes into and off of the wafer.

Fig. 6 Positive surface potentials for 9200 and 9500 implanters with a 60keV As beam at 16mA with and without electron shower operation.

Fig. 7 Multi-component charge source model of ion beam.

Fig. 8 Positive charge signal as a function of load resistance for the 9500 and 9200 implanters with a 16mA As beam showing the current source-like behavior of the beam plasma for low load impedance and voltage source-like characteristics for higher load impedance. The effect of the charge control system operation is to reduce the charging signals for even the highest sensitivity devices to close to the +5V resolution threshold used for this investigation.

Fig. 9 J-V characteristics measured on the edge and center of a wafer implanted with a "raw" 16mA As beam without the Plasma Flood System. The tunneling current characteristics for SiO_2 predict oxide stress currents of $\approx 4\text{mA}/\text{cm}^2$ at the wafers edge and no tunneling for 110\AA oxides near the center on the wafer.

Contact author : Michael Current

Applied Materials, MS0907, 3050 Bowers Ave. Santa Clara, CA 95054 USA

tel:(408)-235-4450;fax:(408)-986-2833;

e-mail:Michael_Current%AMAT@MCIMail.com

Evolution of Electron Showers for Ion Implantation

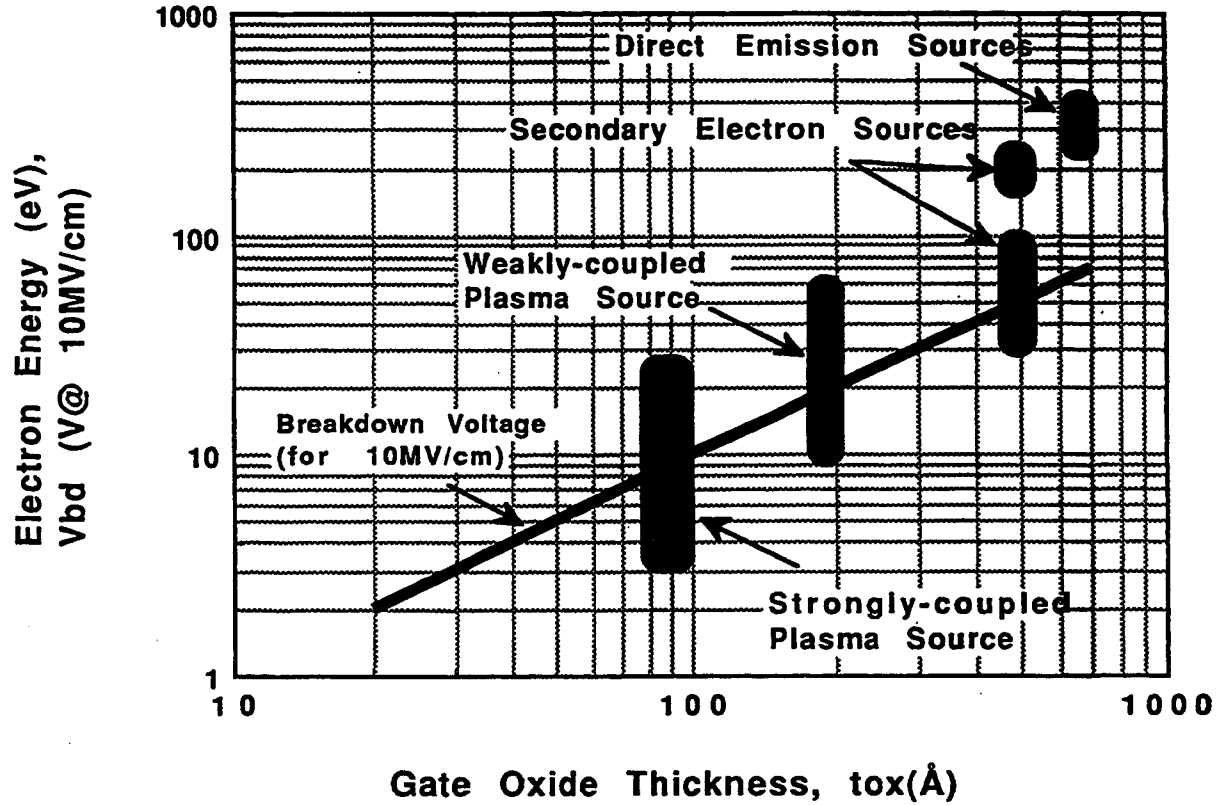


Fig. 1 Intrinsic breakdown voltage for gate oxide films and typical electron energy distributions for sequential generations of electron shower technologies.

Beam Plasma-Device Surface Charge Exchange Mechanisms

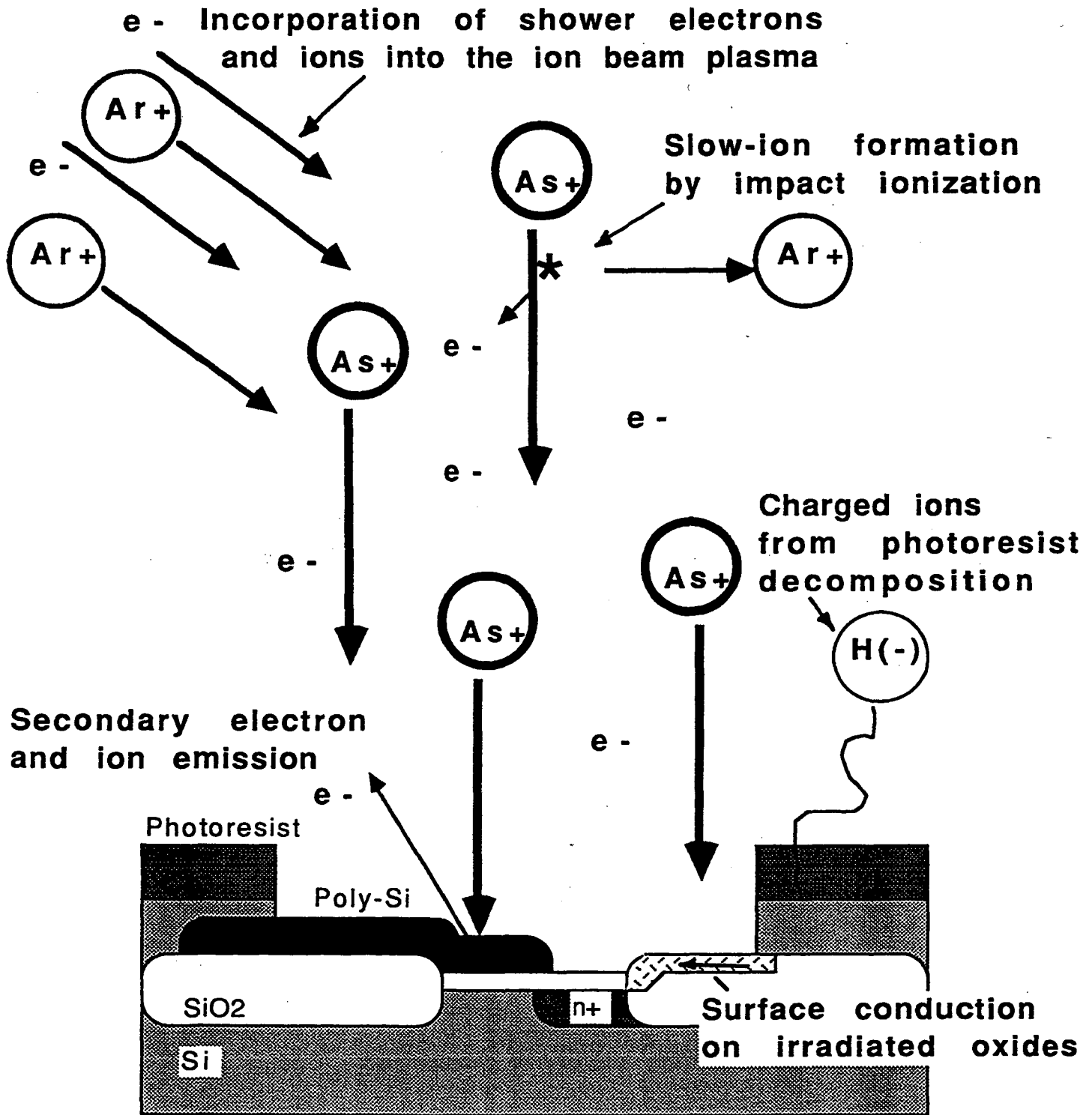


Fig. 2 Charge exchange mechanisms on wafer surfaces and in ion beams.

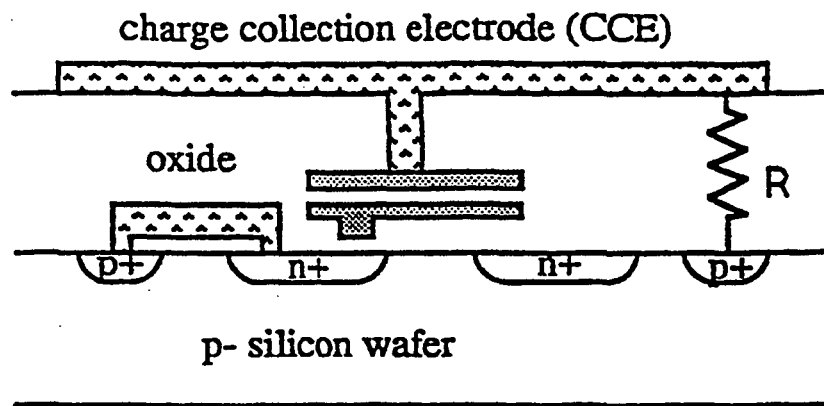


Fig. 3. CHARM-2 EEPROM-based sensor device with resistor load for charge flux measurements.

**CHARM-2 Current Sensitivity Ranges
(0.24mm² collection electrode)**

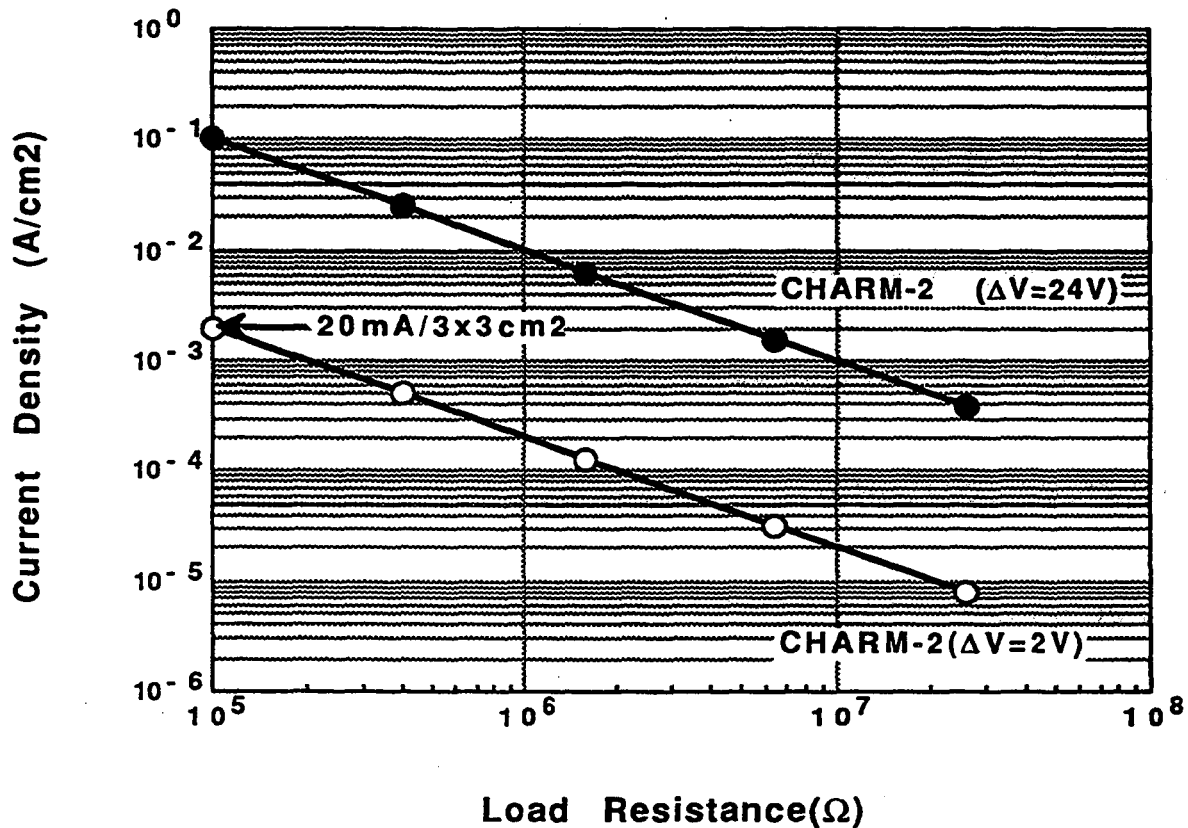
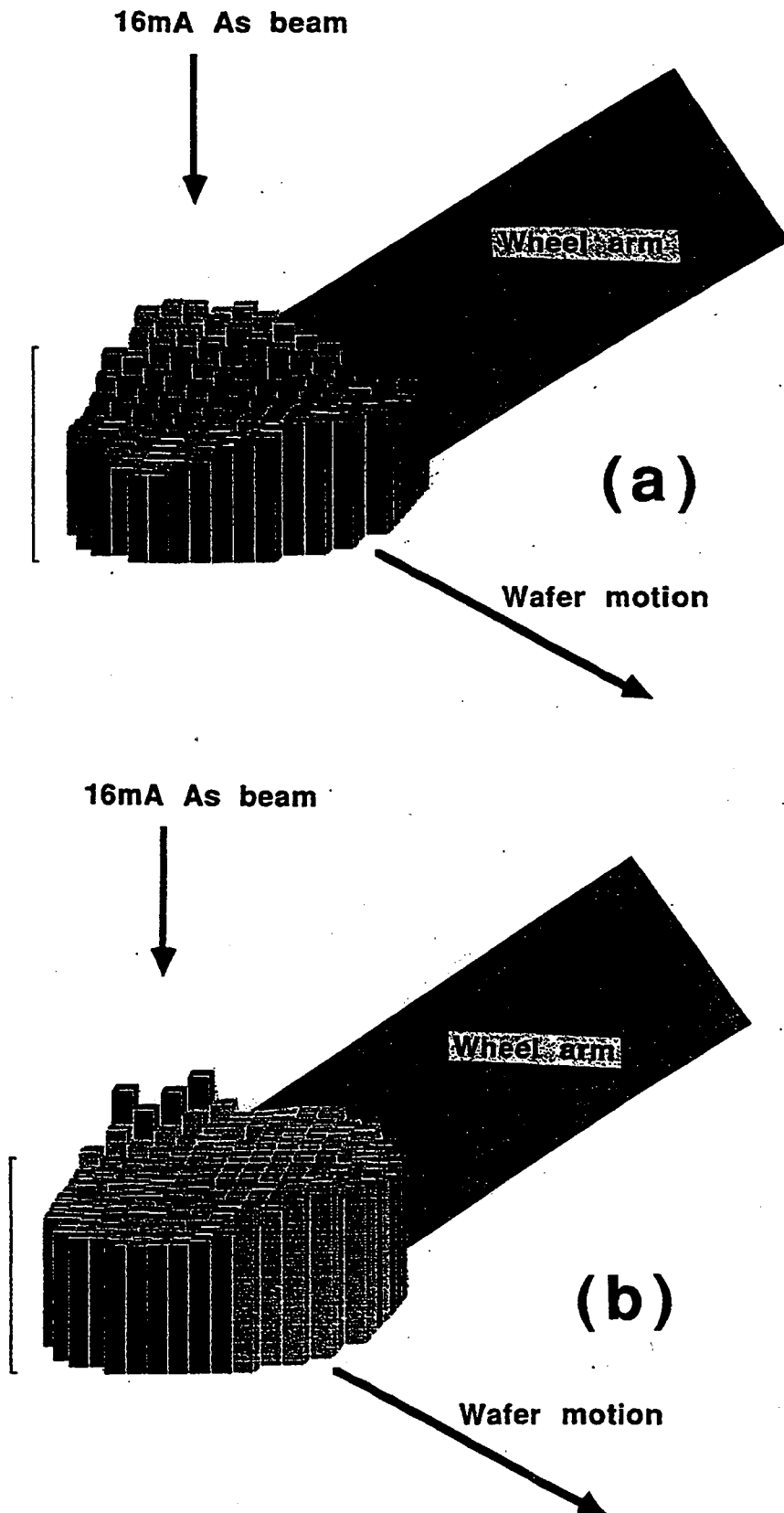


Fig. 4 Charge flux density sensitivity ranges for CHARM-2 sensors for 2 and 24V voltage drops along poly-Si load resistors between charge collection electrodes and Si substrate (for 0.24mm² electrodes).



15

Fig. 5 Wafer maps of positive potential signal from CHARM-2 sensors for 16mA, 60keV As beams from a 9500 implanter. The surface potential for the “raw” As beam (no electron shower) (a) is 11.79 ± 2.74 V and with the Plasma Flood Source (b) is 6.74 ± 0.636 . Note the transient effects that are resolved in these maps in the regions where the beam passes into and off of the wafer.

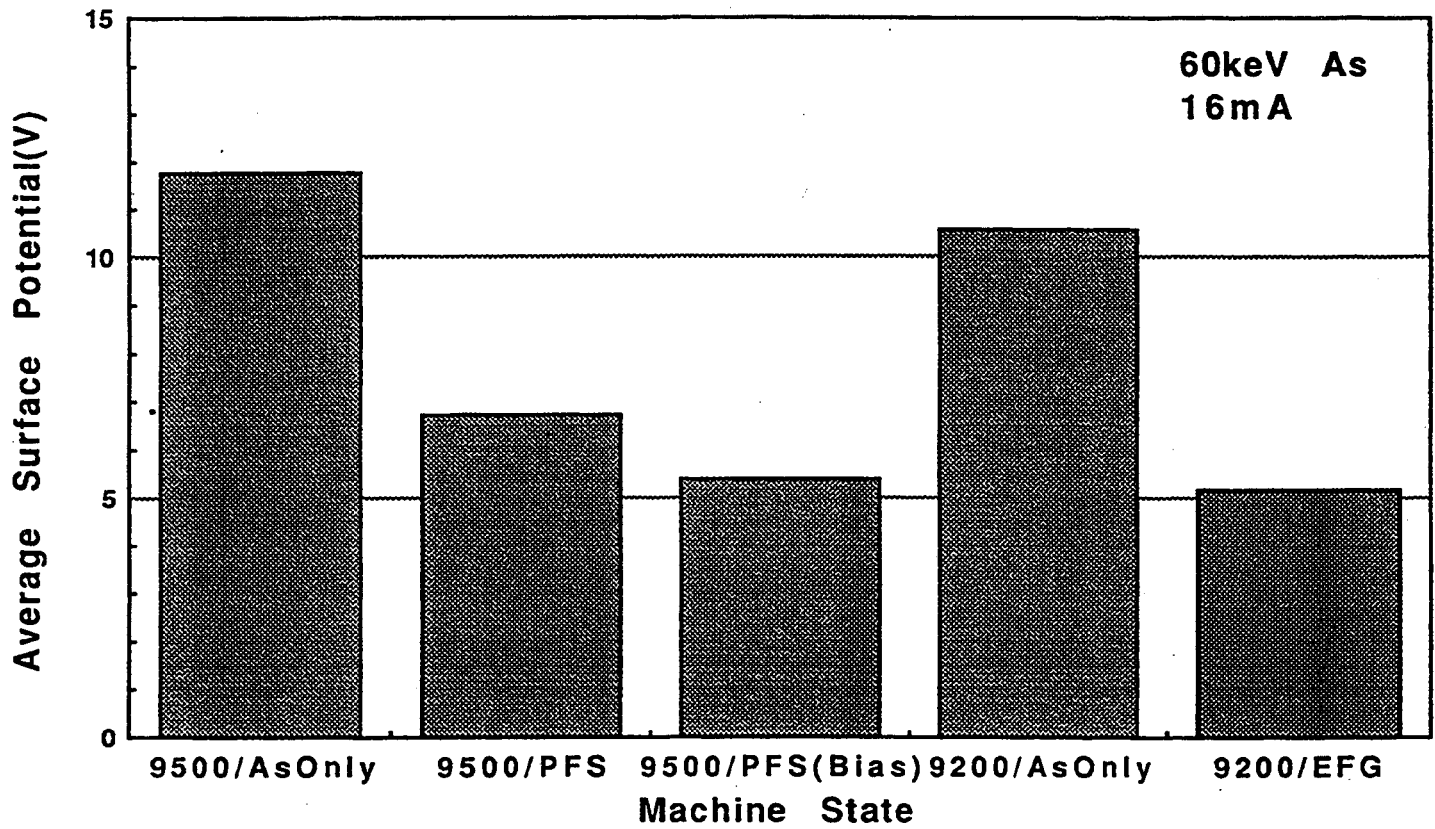


Fig. 6 Positive surface potentials for 9200 and 9500 implanters with a 60keV As beam at 16mA with and without electron shower operation.

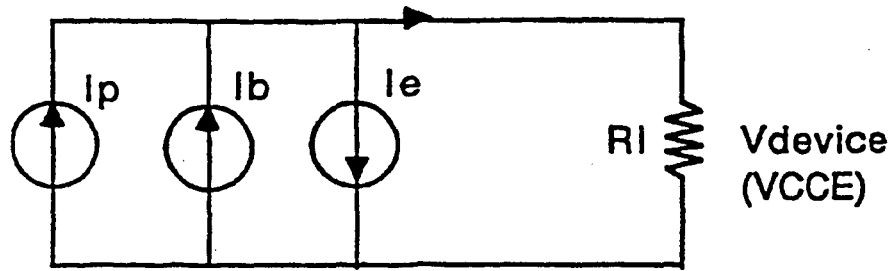


Fig. 7 Multi-component charge source model of ion beam.

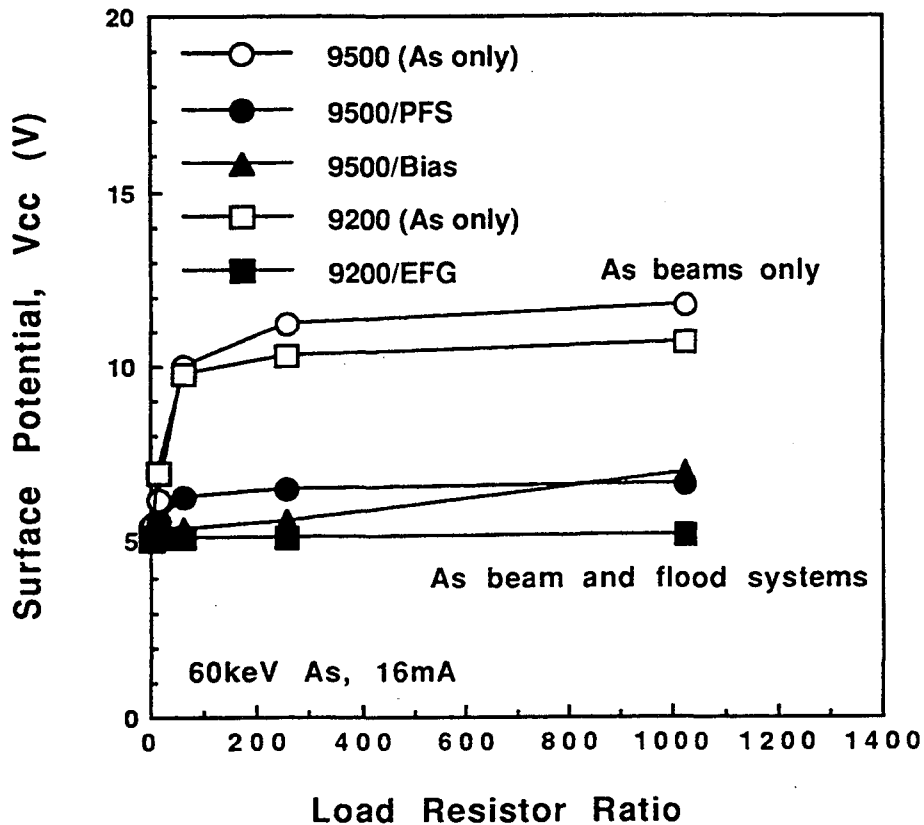


Fig. 8 Positive charge signal as a function of load resistance for the 9500 and 9200 implanters with a 16mA As beam showing the current source-like behavior of the beam plasma for low load impedance and voltage source-like characteristics for higher load impedance. The effect of the charge control system operation is to reduce the charging signals for even the highest sensitivity devices to close to the +5V resolution threshold used for this investigation.

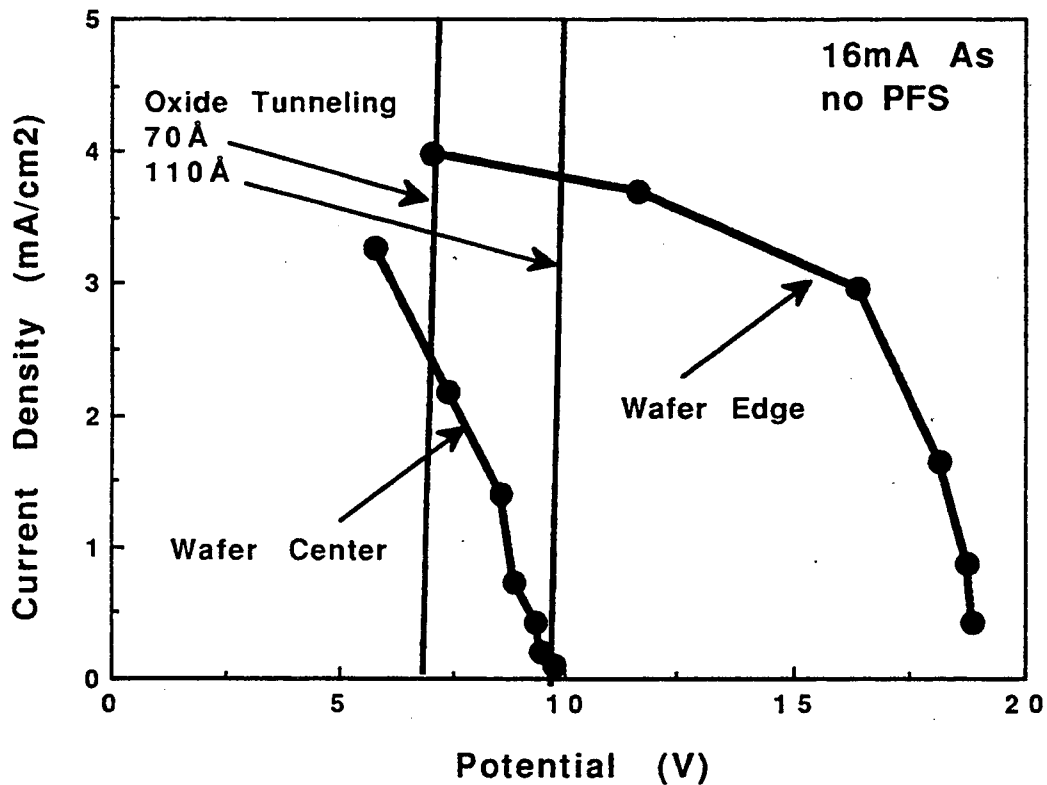


Fig. 9 J-V characteristics measured on the edge and center of a wafer implanted with a "raw" 16mA As beam without the Plasma Flood System. The tunneling current characteristics for SiO₂ predict oxide stress currents of $\approx 4\text{mA/cm}^2$ at the wafers edge and no tunneling for 110Å oxides near the center on the wafer.

LAWRENCE BERKELEY LABORATORY
UNIVERSITY OF CALIFORNIA
TECHNICAL AND ELECTRONIC
INFORMATION DEPARTMENT
BERKELEY, CALIFORNIA 94720